

Received July 6, 2019, accepted July 17, 2019, date of publication July 19, 2019, date of current version August 6, 2019.

Digital Object Identifier 10.1109/ACCESS.2019.2930007

A New Online Temperature Compensation Technique for Electronic Instrument Transformers

ZHENHUA LI^{ID1,2}, Yawei Du^{ID1}, A. ABU-SIADA^{ID3}, (Senior Member, IEEE),

ZHENXING LI¹, AND TAO ZHANG^{ID1}

¹College of Electrical Engineering and New Energy, China Three Gorges University, Yichang 443002, China

²Hubei Provincial Key Laboratory for Operation and Control of Cascaded Hydropower Station, China Three Gorges University, Yichang 443002, China

³Department of Electrical and Computer Engineering, Curtin University, Perth, WA 6000, Australia

Corresponding author: Zhenhua Li (lizhenhua1993@163.com)

This work was supported in part by the National Natural Science Foundation of China under Grant 51507091, in part by the Key Project of Science and Technology Research Plan of Education Department of Hubei under Grant D20181204, and in part by the China Three Gorges University through the Research Fund for Excellent Dissertation, under Grant 2019SSPY051.

ABSTRACT Electronic instrument transformers are expected to play a significant protection and control role in the future smart grids. This paper aims at improving the performance and accuracy of electronic instrument transformers that are replacing the conventional current and potential transformers in the future digital substations. One of the main issues associated with the electronic instrument transformer is its poor thermal stability that affects the accuracy of the measurements. In this paper, to overcome this issue, a new wireless temperature measurement and compensation technique is proposed. In this technique, the operating temperature of the electronic transformer is continuously monitored and its impact on the measurements is compensated in real-time. The experimental results reveal that the proposed technique can effectively improve the thermal stability and measurement accuracy of the electronic instrument transformers.

INDEX TERMS Electronic instrument transformers, wireless temperature measurement, thermal stability, digital substations.

I. INTRODUCTION

Electronic instrument transformer has been given much attention during the last few years as a cost-effective asset to replace the classic magnetic core-based instrument transformers due to its several advantages that include wide band width and large dynamic range [1]–[4]. However, due to the diverse sensing principles within the electronic instrument transformer, it is reported to be of poor thermal stability that affects its measurement accuracy [5]–[9]. Unlike the traditional electromagnetic transformer that exhibits better temperature performance and generally does not require temperature compensation, the electronic instrument transformer must employ an effective temperature compensation technique. The research on temperature compensation is mainly focusing on the optical-based electronic transformer which has a single measurement function [10]–[12]. There are other

electronic transformers with new measuring principles that are also influenced by the operating temperature variations. This includes electronic transformer based on Rogowski coil and coaxial capacitor that can simultaneously measure the voltage and current signals [13]–[15]. Therefore, it is necessary to develop a cost-effective technique to monitor the temperature of an operating electronic combined instrument transformer and compensate the temperature effect in real-time to improve its overall thermal stability and enhance the measurement accuracy. A few studies can be found in the literatures on the temperature compensation of electronic transformers [16]–[19] in which the proposed temperature measurement techniques include infrared [20], [21], fiber Bragg grating [22]–[25] and wireless measurement [26], [27]. The infrared thermometry is susceptible to the complex internal structure of the electronic instrument transformer and has a low accuracy measurement. On the other hand, while the insulation of the fiber Bragg grating can be realized, the fiber can be easily broken and its surface is prone to

The associate editor coordinating the review of this manuscript and approving it for publication was Avishek Guha.

contamination, which results in a creepage along the fiber surface and reduction in the insulation performance of the system. The wireless temperature measurement method is easy to realize in electronic instrument transformer; however, the power supply at the high voltage side is a challenge and the interference with the surrounding electromagnetic field along with the adverse effect of operating temperature reduce the accuracy of measurements. References [28]–[30] present the application of wireless temperature measurement alarm system in medical and greenhouse temperature management. Once the temperature of the equipment is abnormal, the system can be automatically alarmed remotely to eliminate accidents in real time. For the temperature compensation of electronic transformers, there are relatively few related studies. References [31]–[33] present temperature compensation techniques for a closed-loop all fiber current transformer and fiber Bragg grating AC current transformer, which improve the test accuracy of the system in the full temperature range. However, these temperature compensation techniques mainly focus on sensor temperature performance analysis without giving much attention to the temperature measurement technology itself. This paper focuses on the key technologies and compensation techniques in wireless temperature measurement system.

In view of the deficiency of the main temperature measurement methods presented above, a new wireless temperature measurement system is proposed in this paper for a designed electronic combined instrument transformer. The temperature measuring system comprises a transmission module mounted at the high voltage side of the instrument transformer, a receiving module that is placed at the low voltage side and a monitoring software dashboard in the upper computer. In order to eliminate the interference with the surrounding electromagnetic field, an anti-interference method is developed for both hardware and software, which guarantees the accuracy of the temperature data that are compensated to improve the measurement accuracy of the electronic instrument transformer. The proposed temperature measurement system can be employed in a wide range of applications including power system protection, control and condition monitoring of the critical assets within the transmission and distribution networks.

II. BASIC STRUCTURE OF ELECTRONIC TRANSFORMER

The basic structure of the electronic combined instrument transformer shown in Fig. 1 comprises a Rogowski coil sensor to realize current measurement and a coaxial capacitor sensor for voltage measurement. The current and voltage sensors are used for measurement and protection at the same time. These sensors exhibit high thermal stress due to the large current passing through the main conductor. Furthermore, the dynamic change in the environmental temperature will have adverse effects on the measurement accuracy of these sensors. Therefore, to maintain high measurement accuracy for the current and voltage sensors, it is necessary to monitor the internal operating temperature of the electronic instrument

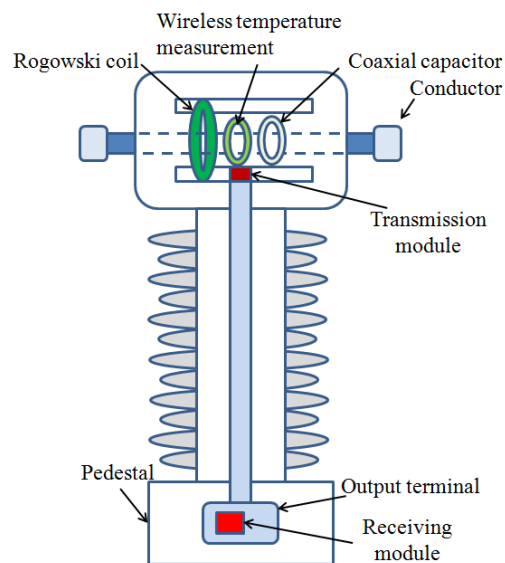


FIGURE 1. Basic structure of electronic combined instrument transformer.

transformer to compensate its adverse impact on the measurement accuracy of the sensor. The operating temperature of electronic transformers is usually within the range -40°C to $+50^{\circ}\text{C}$. Within this temperature range, the measurement error of the electronic transformer should not exceed $\pm 0.2\%$.

III. DESIGN OF THE PROPOSED SYSTEM

The proposed temperature measuring system is shown in Fig. 2. The system consists of a transmission module, a receiving module and a monitoring software in the upper computer. The transmission module is installed at the high voltage side of the transformer as shown in Fig. 1 and is used to measure the surrounding temperature of the sensors and transmit the measured data to the receiving module via a wireless transmission. The current and voltage measurements of the Rogowski coil and the coaxial capacitor are also collected by the transmission module and transmitted to the receiving module. Optical fiber is used to connect the receiving module and the merging unit of the electronic instrument transformer while output data from the merging unit are transmitted to the upper computer through a network cable using IEC 61850-9-2 communication protocol. The transmission module side comprises a special power supply coil circuit, a temperature sensor, a single chip microcomputer (SCM) control circuit and a wireless transmitter.

On the other hand, the receiving module that is mounted at the pedestal consists of a SCM control circuit and a wireless receiver. The detailed designs of these components are elaborated below.

A. DESIGN OF THE TRANSMISSION MODULE

The transmission module consists of temperature sensor, power processing and energy storage (lithium battery), SCM and wireless transceiver circuit, as shown in the schematic diagram of Fig.3.

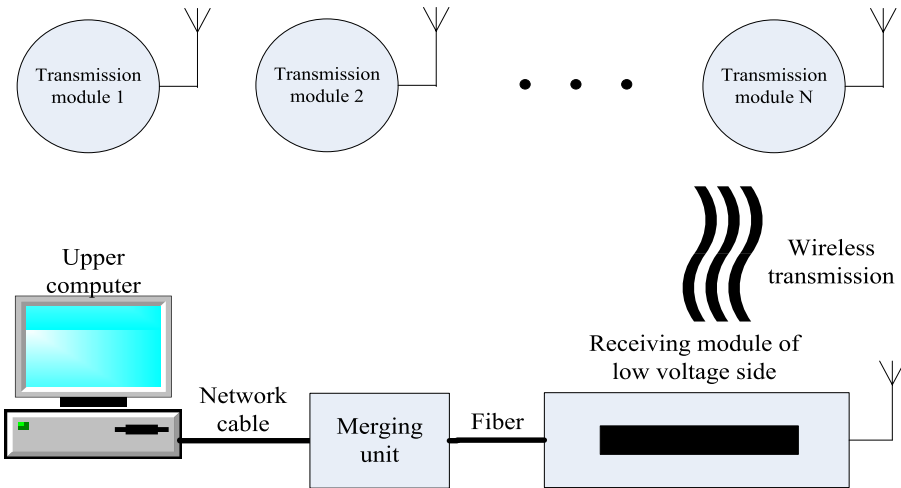


FIGURE 2. Main structure of the proposed wireless temperature measurement system.

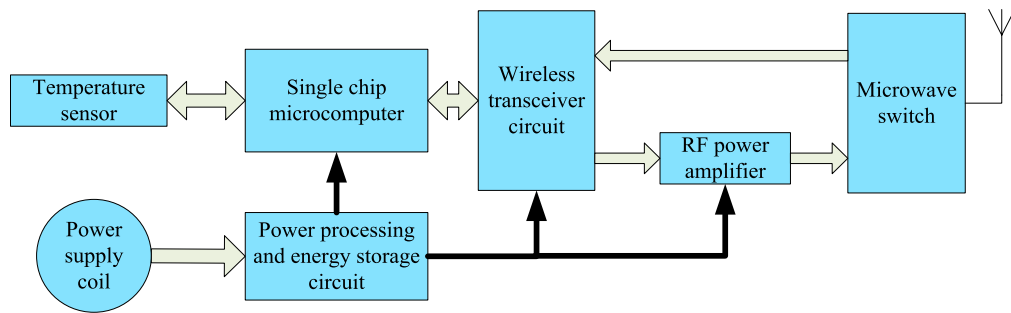


FIGURE 3. Main components of the transmission module at the high voltage side.

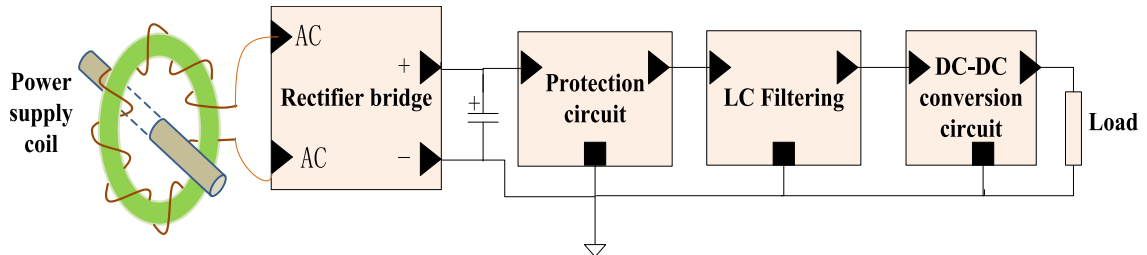
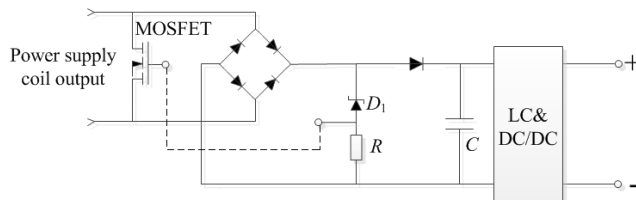
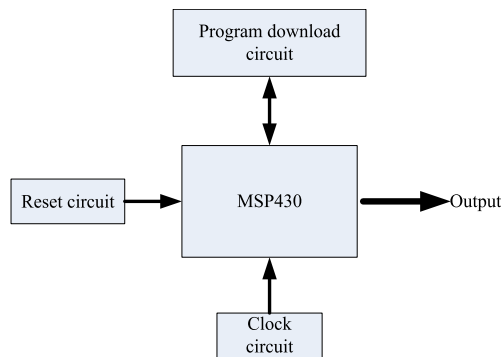


FIGURE 4. Schematic diagram of the power supply coil circuit.

A digital temperature sensor DS18B20 with a range of -55°C to $+125^{\circ}\text{C}$ is used for temperature measurement. The electronic components in the transmission module are energized using a special power supply coil of 3.3V output voltage and an energy storage circuit. According to the design requirements, the current variation range of the transformer is 50A to 1.25kA. As the power supply should be functioning outside this range, the energy storage circuit supplies the required power when the current is less than 50A while the power supply coil is functioning when the current is larger than 50A to provide the required power and charge the lithium battery at the same time. Using saturation characteristic of

the power supply coil, the power supply circuit can convert the current signal within the designated range into a voltage signal of about 3.3V. The operating principle diagram of the power supply coil circuit is shown in Fig.4.

In Fig. 4, the output of the power supply coil is transmitted to a full wave rectification circuit that converts the input signal into DC voltage. The level of the output DC voltage is regulated to 3.3V using LC filtering along with DC-DC conversion circuits. As the rectified voltage increases with the increase in the primary current, a protection circuit as shown in Fig.5 is also used to protect the subsequent DC-DC conversion circuit. In Fig.5, if the voltage across the diode

**FIGURE 5.** Schematic diagram of the protection circuit.**FIGURE 6.** Peripheral circuit of MSP430F123 as a single chip microcomputer.

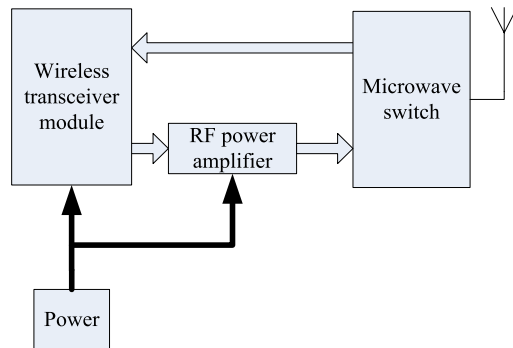
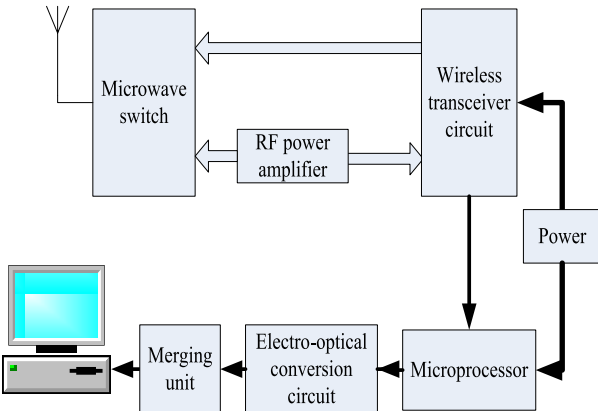
D_1 is greater than its operating voltage, the metal-oxide-semiconductor field-effect transistor (MOSFET) will operate in the triode region and the secondary output of the power supply coil will be shorted, then the coil will not charge the capacitor C.

A LP2950CDT-3.3G is used as the DC-DC conversion chip, which can realize a DC output of 3.3V. MSP430F123 microprocessor is employed to control the temperature sensor, receive data from the sensors, and control the wireless transceiver circuit, according to the application environment and requirements of the temperature measurement system. The peripheral circuit includes SCM, reset circuit, clock circuit and program download circuit as shown in Fig.6. The transmitter circuit at the high voltage side is facilitated to transmit the measured data wirelessly to the receiver that is mounted at the low voltage side of the electronic instrument transformer.

At present, the main technologies of short-range wireless communication technologies include ZigBee, Nordic 2.4G, Wi-Fi, 3G/HSDPA, WiMAX, UWB, and Bluetooth. These main wireless communication methods usually adopt 2.4GHz frequency band for short-range communication [34]. Considering cost, power consumption and transmission rate, nRF24L01 chip is utilized for the wireless transmission circuit. The circuit contains wireless transceiver module, RF power amplifier and microwave switch as shown in Fig.7.

B. DESIGN OF RECEIVING MODULE

The temperature data of the transmission module is transmitted using wireless transmission to the receiving module. An optical fiber is used to connect the receiving module

**FIGURE 7.** Principle diagram of wireless transceiver circuit.**FIGURE 8.** Detailed diagram of the receiving module.

and the merging unit. Data from merging unit are transmitted to the upper computer through a network cable using IEC 61850-9-2 communication protocol. The receiving module consists of power supply, microprocessor, wireless transceiver circuit and electro-optical conversion circuit as shown in Fig.8.

The MSP430F147 microprocessor in Fig. 8 has 32k FLASH and 1k RAM capacity. The concept of the wireless transceiver circuit of the receiving module is the same as that of the transmission module, while it is set to receiving mode in the software design. An external antenna is used to enhance the sensitivity of the receiving module.

It is to be noted that all hardware components used in developing the hardware model are of average operational life of 20 years based on manufacturer data. So, it is expected that the life of the proposed hardware model to be the same unless external accelerating aging factors contribute in decreasing this expected life. Aging assessment of this model requires further in-depth analysis. The daily power consumption of the developed model is approximately in the range 15 - 20 mW.

C. SOFTWARE DESIGN

The developed software includes software of the SCM and the monitoring software on the upper computer. The software function in the SCM is mainly to perform the

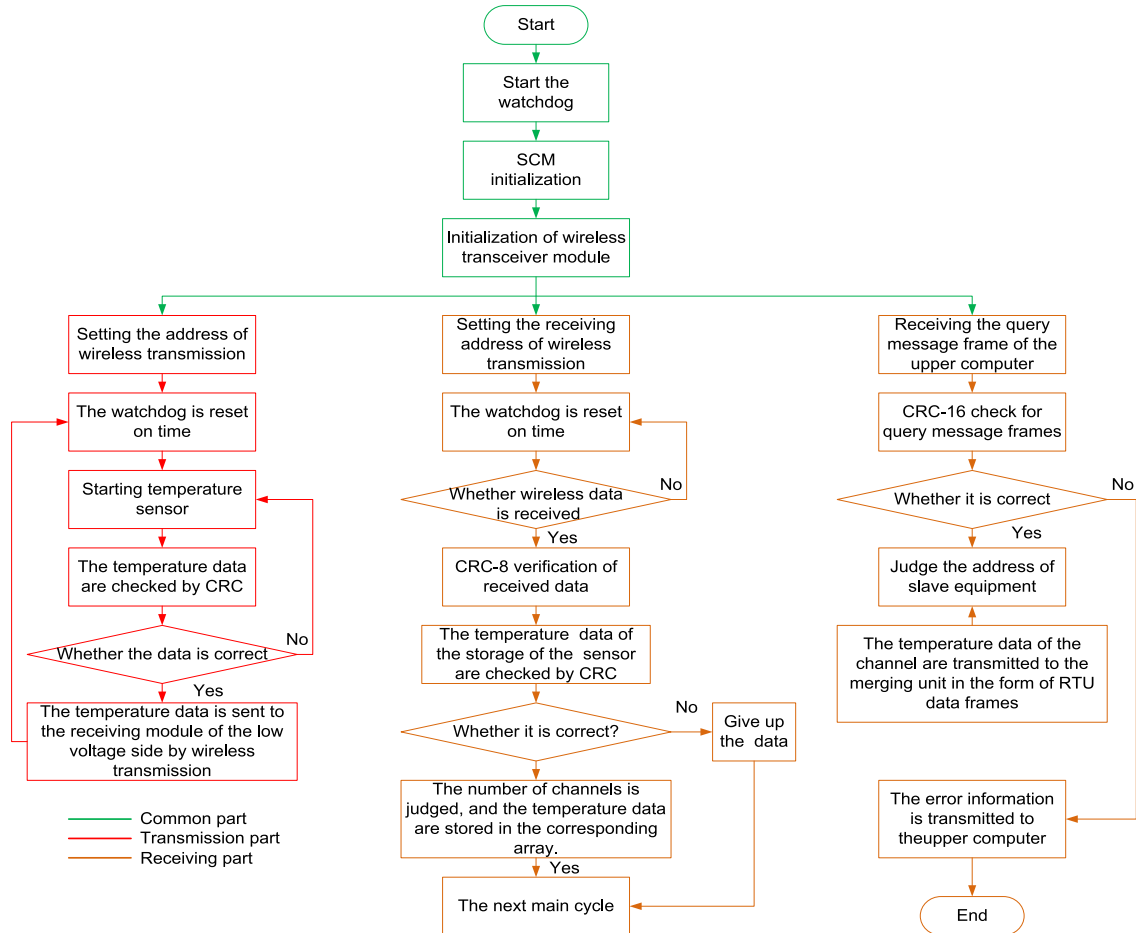


FIGURE 9. Flow chart of the SCM and receiving circuit software.

communications between microprocessor, temperature sensor, wireless transceiver module, and the upper computer. The software in the upper computer is used to process the temperature data and realize real-time monitoring of the temperature within the electronic transformer.

1) SOFTWARE OF SCM AND RECEIVING CIRCUIT

The developed software flow chart shown in Fig.9 interacts with the temperature sensor and the wireless transceiver module. Due to the expected harsh electromagnetic operating environment, the MSP430 chip may experience malfunction and its program may not work properly. To resolve the issue and to prevent loss of control, a watchdog timer is included in the software program. The system will be automatically reset when the program is running abnormally due to interference. In addition, cyclic redundancy check (CRC) is adopted to verify the data of temperature sensor and determine the correctness of the temperature measurement data.

The function of the software at the receiving circuit is to obtain the temperature data from the transmitter and communicate it to the merging unit through the optical fiber with the MODBUS protocol. The setup of the watchdog timer,

initialization of MSP430 and the wireless transceiver module in this program are basically the same as those in the SCM software.

2) SOFTWARE OF THE UPPER COMPUTER

The monitoring software of the upper computer is developed using Labview. The software comprises three main parts: software interface between the upper computer and the receiving module, query-response message frame processing in IEC 61850-9-2 protocol, display and preservation of temperature data. The software dashboard is shown in Fig.10 which can simultaneously display up to six channels of temperature data.

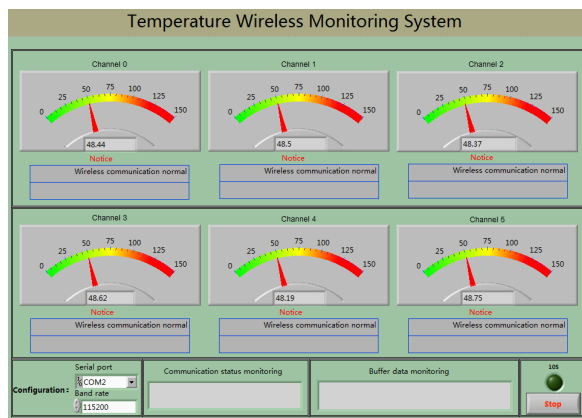
IV. PROPOSED SYSTEM TESTING AND APPLICATION

A. ACCURACY TEST

In this test, a temperature control box is used to carry out the accuracy assessment of the proposed system in measuring a wide range of temperatures. Six temperature sensors along with the developed transmission modules are placed into the temperature control box. At the same time, a standard FLUKE multi-meter with k-type thermocouple is utilized

TABLE 1. Results of the proposed system accuracy test.

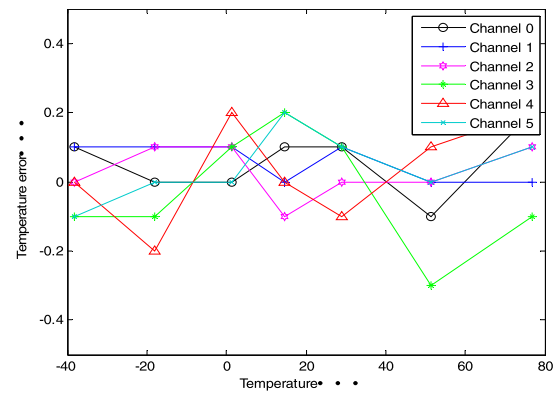
Measurement Approach*	Control box temperature (°C)						
	Temperature 1	Temperature 2	Temperature 3	Temperature 4	Temperature 5	Temperature 6	Temperature 7
Thermocouple	-38.2	-18.0	1.2	14.5	29.0	51.5	76.8
Channel 0	-38.3	-18.0	1.2	14.4	28.9	51.6	76.6
Channel 1	-38.3	-18.1	1.1	14.5	28.9	51.5	76.8
Channel 2	-38.2	-18.1	1.1	14.6	29.0	51.5	76.7
Channel 3	-38.1	-17.9	1.1	14.3	28.9	51.8	76.9
Channel 4	-38.2	-17.8	1.0	14.5	29.1	51.4	76.6
Channel 5	-38.1	-18.0	1.2	14.3	28.9	51.5	76.7

**FIGURE 10.** Monitoring software dashboard of the upper computer.

to compare the results of the proposed temperature measurement system with. The temperature measuring range of the thermocouple is -55°C to $+400^{\circ}\text{C}$ with accuracy and maximum resolution of $\pm 1.0\%$ and 0.1°C , respectively. The environment temperature in the control box is changed in a wide range while the temperature measurements using the standard thermocouple and the proposed developed system are recorded in Table I. The results reveal the high accuracy of the proposed temperature measurement system. The error between the measured temperature using the 6 channels (channel 0 to 5 in Table I) and that of the standard thermocouple is very small as shown in Fig.11.

B. WIRELESS TRANSMISSION DISTANCE TEST

The distance of wireless transmission is one of the key design features of the proposed wireless temperature measurement system. To assess this criterion in the developed system, unshielded and shielded tests were performed. The unshielded test is carried out in an open field while the shielded test is carried out by placing the transmission module in an aluminum sealed box. Test results are summarized below:

**FIGURE 11.** Percentage error of each channel of the proposed system with respect to the standard thermocouple measurement.

1) UNSHIELDED TEST

Accurate temperature data can be received within a distance of 80 meters between the transmission and receiving modules without any barrier. Beyond this distance, data interruption is taking place. This distance is reduced to 50 meters with any kind of barriers such as a wall between the two modules.

2) SHIELDED TEST

Accurate temperature data can be received within 50 meters without any barrier, which is reduced to 30 meters with a barrier between the two modules.

It is worth mentioning that the receiving module is placed at the transformer base while the transmission module is installed at the top high voltage side. Hence, the separation distance is much less than 30 meters which meets the application requirement. Other wireless transmission communication technology such as LTE module that has longer transmission distance and wider range of applications, can be also employed in the developed system.

C. PRACTICAL APPLICATION

The developed wireless temperature measurement system shown in Fig.12(a) is used within the electronic instrument

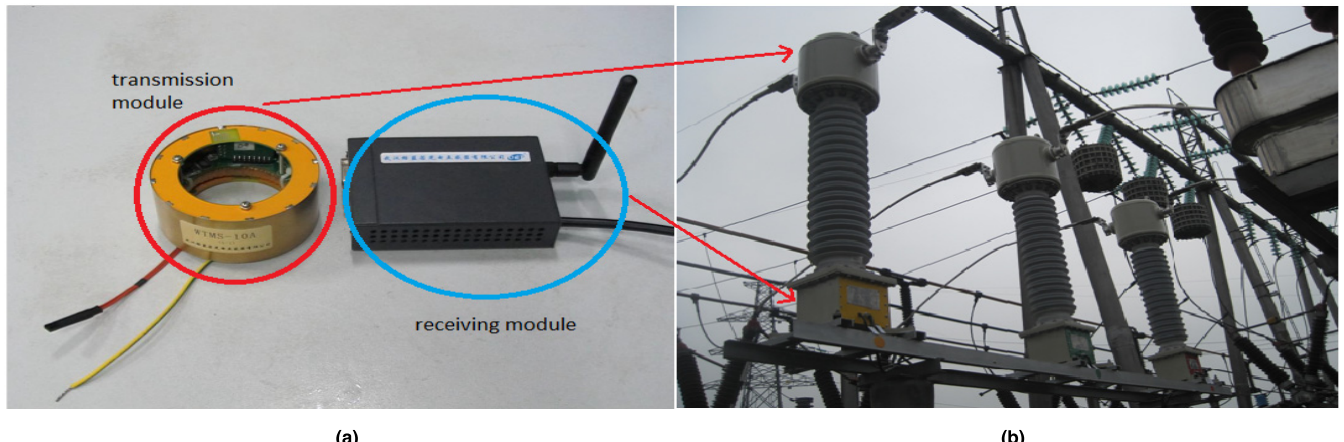


FIGURE 12. Practical application of the developed system (a) Wireless temperature measurement system, (b) Electronic instrument transformer.

TABLE 2. Temperature Compensation Effect Test for Current.

Using Standard CT (% of Rated Current)	Temperature (°C)	Before Compensation		After Compensation	
		Ratio Error (%)	Phase Error (°)	Ratio Error (%)	Phase Error (°)
1949.2 (97.46)	15.2	-0.0426	-0.132	-0.0127	0.178
1914.6 (95.73)	50.4	0.0977	-4.266	-0.0265	-1.066
1909.4 (95.47)	50.3	0.0928	-3.916	-0.0219	-1.116
1934.6 (96.73)	15.1	-0.0579	-0.035	-0.0292	-0.007
1935.4 (96.77)	-25.4	-0.0859	1.318	-0.0183	0.877
1934.2 (96.71)	-25.4	-0.0875	1.558	-0.013	0.653
1933(96.65)	-25.6	-0.077	2.063	-0.0227	0.786
1982.4 (99.12)	-38.9	-0.2259	7.466	-0.0458	0.876
1987 (99.35)	-39.2	-0.1866	6.722	-0.0447	0.881
1978.6 (98.93)	-39.1	-0.2003	6.666	-0.0384	0.680
1943.3 (97.165)	15.0	-0.0438	-0.102	-0.0163	-0.013

transformer shown in Fig.12(b). The transformer rated voltage and current are 110kV and 2kA, respectively. The temperature performance of the electronic transformer is tested and the measured current and voltage data without the compensation of the temperature effect are recorded in Tables II and III, respectively. In this test, the transformer is placed in a large temperature-controlled cabinet at which the surrounding temperature can be controlled in a wide range from -40°C to 70°C . The developed system can measure the temperature at every 5 seconds. On the other hand, the voltage and current sampling frequency of the electronic instrument transformer is usually 4 kHz or higher. In Tables II and III, the percentage magnitude error and the phase error in the measured current and voltage signals are calculated using the following formula:

$$\text{Percentage magnitude error} = \frac{X_T - X_S}{X_S} \times 100\% \quad (1)$$

$$\text{Phase error} = \varphi_T - \varphi_S \quad (2)$$

where, X_T and X_S are the root mean square voltage or current measured using the electronic instrument transformer and a standard current (CT)/ potential (PT) transformers, respectively while φ_T and φ_S are the corresponding phase angles that are calculated using Fast Fourier Transform. The test was conducted in accordance to the IEC standards [35], [36]. It can be seen from Table II that by reducing the temperature within the temperature-controlled cabinet from 50.4°C to -39.2°C , the current measured using the standard CT is increasing by 3.8% which is attributed to the reduction in the conductor resistance with the decrease in the surrounding temperature. On the other hand, a voltage variation of 1.3% is noticed in the standard PT reading when the temperature is reduced within the same range. Due to its sensitivity to temperature variation, the reading of the electronic instrument transformer exhibits an error in both magnitude and angle of the measured current and voltage signals when compared with the reading of the standard CT and PT as shown in columns 3 and 4 in Tables II and III; respectively.

TABLE 3. Temperature Compensation Effect Test for Voltage.

Voltage (kV) Using standard PT (% of Rated Voltage)	Temperature (°C)	Before Compensation		After Compensation	
		Ratio Error (%)	Phase Error (')	Ratio Error (%)	Phase Error (')
61.5 (96.84)	15.2	-0.012	-0.984	-0.0084	-0.224
60.9 (95.89)	50.4	0.1636	-2.114	0.0444	-0.44
60.7 (95.58)	50.3	0.158	-2.05	0.0439	-0.399
61.4 (96.68)	15.1	-0.0077	0.881	-0.0036	-0.232
61.4 (96.68)	-25.4	-0.1873	2.311	-0.0222	0.813
61.4 (96.68)	-25.4	-0.1814	2.109	-0.0303	0.797
61.4 (96.68)	-25.6	-0.1914	2.607	-0.0285	0.788
61.7 (97.15)	-38.9	-0.6309	3.725	-0.0411	1.596
61.8 (97.31)	-39.2	-0.6271	4.376	-0.0497	1.61
61.7 (97.15)	-39.1	-0.6047	5.556	-0.0483	1.575
61.4 (96.68)	15.0	-0.0146	-0.323	-0.0045	-0.212

It can be observed that without compensation, some current and voltage measurements will exhibit error more than the standard permissible limit of $\pm 0.2\%$ as highlighted in bold font in Tables II and III. With the proposed temperature compensation, the ratio error in all current and voltage reading has been reduced to a level less than 0.05%.

Even though the error in the electronic instrument transformer reading with the variation of environment temperature seems to be insignificant, this small error may lead to malfunction in the protection and control systems. For example, at -38.9°C , the error in the RMS current measured by the electronic instrument transformer was found to be -0.2259% . This current is less than the actual current measured by the standard CT. If the protection relay setting was above the reading revealed by the electronic current transformer, the protection system will not be activated due to such error. Hence it is essential to compensate the temperature effect on the measurement accuracy of the electronic instrument transformers as will be elaborated below.

Assuming at a given temperature T , the compensation coefficients for the current magnitude and phase are respectively denoted by r_C and p_C and by r_V and p_V for the voltage magnitude and phase. The least square method is used to calculate the fitting curves of the percentage magnitude error and phase error in Tables II and III with the temperature as per Eqs.3-6 below:

$$r_C = 2.191 \times 10^{-6} T^3 - 4.343 \times 10^{-5} T^2 - 7.519 \times 10^{-4} T - 0.0365 \quad (3)$$

$$p_C = -8.110 \times 10^{-5} T^3 + 0.0023 T^2 + 0.0202 T - 0.6414 \quad (4)$$

$$r_V = 5.708 \times 10^{-6} T^3 - 2.227 \times 10^{-4} T^2 - 7.010 \times 10^{-4} T - 0.0321 \quad (5)$$

$$p_V = -1.872 \times 10^{-5} T^3 + 7.999 \times 10^{-4} T^2 - 0.0441 T + 0.4981 \quad (6)$$

These equations are used to compensate the effect of temperature variations on the output current and voltage readings of the electronic current transformer. For example, the following formula is used to compensate the effect of temperature variations on the magnitude of the root mean square current measured by the electronic current transformer:

$$I_{TH} = \left(1 - \frac{r_C}{100}\right) \times I_{TB} \quad (7)$$

where I_{TH} is the compensated current reading and I_{TB} is the reading before compensation.

As can be seen in the compensated data in Tables II and III, the wireless temperature measurement system can measure the temperature and perform accurate compensation to correct the electronic instrument transformer reading. For example, at a temperature of -38.9°C , the error in the RMS current measured by the electronic instrument transformer is reduced from -0.2259% to only -0.0458% . This reveals the robustness of the proposed compensation technique.

V. CONCLUSION

This paper designs and implements a new wireless temperature measurement and compensation system that resolves the poor thermal stability issues associated with electronic instrument transformers and improves their measurement accuracy. The proposed technology consists of a transmitter mounted at the high voltage side, receiving unit mounted at the low voltage side and an upper computer software monitoring system. Considering the harsh electromagnetic operating environment of the transformer high voltage side, an anti-interference design is considered in the developed hardware and software systems to effectively ensure the accuracy of the temperature

measurement data. Accuracy test and field application of the developed system reveal that it can accurately measure the temperature within the electronic instrument transformer and compensate the effect of temperature variations on its thermal stability and measured current and voltage data. The proposed temperature measurement and compensation system is modular and is easy to implement within existing electronic instrument transformers.

REFERENCES

- [1] H. Wu, C. Jiao, X. Cui, X. Liu, and J. Ji, "Transient electromagnetic disturbance induced on the ports of intelligent component of electronic instrument transformer due to switching operations in 500 kV GIS substations," *IEEE Access*, vol. 5, pp. 5104–5112, 2017.
- [2] S. Kucuksari and G. G. Karady, "Experimental comparison of conventional and optical current transformers," *IEEE Trans. Power Del.*, vol. 25, no. 4, pp. 2455–2463, Oct. 2010.
- [3] Z. H. Li, Y. Du, A. Abu-Siada, G. Bao, J. Yu, T. Hu, and T. Zhang, "An online calibration system for digital input electricity meters based on improved nuttall window," *IEEE Access*, vol. 6, pp. 7126–71270, 2018.
- [4] G. I. Volovich, "The influence of internal noise on electronic current transformer error," *Meas. Techn.*, vol. 59, no. 2, pp. 164–169, 2016.
- [5] A. Moradi and S. M. Madani, "Technique for inrush current modelling of power transformers based on core saturation analysis," *IET Gener. Transmiss. Distrib.*, vol. 12, no. 10, pp. 2317–2324, May 2018.
- [6] H. Waqas, A. H. Qureshi, M. Shahzad, "Effect of firing temperature on the electromagnetic properties of electronic transformer cores developed by using nanosized Mn-Zn ferrite powders," *Acta Metallurgica Sinica (English Lett.)*, vol. 28, no. 2, pp. 159–163, Feb. 2015.
- [7] Y. S. Li, W. Zhang, X. Liu, and J. Liu, "Characteristic analysis and experiment of adaptive fiber optic current sensor technology," *Appl. Sci.*, vol. 9, no. 2, p. 333, Jan. 2019.
- [8] H. Xiao, B. Liu, S. Wan, and Y. Zhao, "Temperature error compensation technology of all-fiber optical current transformers," *Autom. Electr. Power Syst.*, vol. 35, no. 21, pp. 91–95, Nov. 2011.
- [9] Z. Li, Y. Tao, A. Abu-Siada, M. A. S. Masoum, Z. Li, Y. Xu, and X. Zhao, "A new vibration testing platform for electronic current transformers," *IEEE Trans. Instrum. Meas.*, vol. 68, no. 3, pp. 704–712, Mar. 2019.
- [10] K. Bohnert, P. Gabus, J. Nehring, and H. Brandle, "Temperature and vibration insensitive fiber-optic current sensor," *J. Lightw. Technol.*, vol. 20, no. 2, pp. 267–276, Feb. 2002.
- [11] C. Huang, J. Mei, Q. Bu, and L. Su, "FPGA-based adaptive phase-shift compensation method for electronic instrument transformers," *Electr. Power Compon. Syst.*, vol. 45, no. 7, pp. 774–784, 2017.
- [12] M. Leibl, G. Ortiz, and J. W. Kolar, "Design and experimental analysis of a medium-frequency transformer for solid-state transformer applications," *IEEE J. Emerg. Sel. Topics Power Electron.*, vol. 5, no. 1, pp. 110–123, Mar. 2017.
- [13] N. I. Elkalahy, T. A. Kawady, E. M. Esmail, and A. I. Taalab, "Fundamental current phasor tracking using discrete Fourier transform extraction of Rogowski coil signal," *IET Sci., Meas. Technol.*, vol. 10, no. 4, pp. 296–305, Jul. 2016.
- [14] M. Zhang, K. Li, S. He, and J. Wang, "Design and test of a new high-current electronic current transformer with a Rogowski coil," *Metrol. Meas. Syst.*, vol. 21, no. 1, pp. 121–132, Mar. 2014.
- [15] E. P. Suomalainen and J. K. Hallstrom, "Onsite calibration of a current transformer using a Rogowski coil," *IEEE Trans. Instrum. Meas.*, vol. 58, no. 4, pp. 1054–1058, Apr. 2009.
- [16] H. Wang, B. Ju, W. Li, and Z. Feng, "Ultrastable eddy current displacement sensor working in harsh temperature environments with comprehensive self-temperature compensation," *Sens. Actuators A, Phys.*, vol. 211, pp. 98–104, May 2014.
- [17] H. Hu, J. Huang, L. Xia, Z. Yan, and S. Peng, "The compensation of long-term temperature induced error in the all fiber current transformer through optimizing initial phase delay in $\lambda/4$ wave plate," *Microw. Opt. Technol. Lett.*, vol. 61, no. 7, pp. 1769–1773, Jul. 2019.
- [18] D. Filipović-Grčić and B. Filipović-Grčić, "Compensation method for improving capabilities of AC current test equipment," *Electr. Power Syst. Res.*, vol. 121, pp. 170–175, Apr. 2015.
- [19] K. Sasaki, M. Takahashi, and Y. Hirata, "Temperature-insensitive sagnac-type optical current transformer," *J. Lightw. Technol.*, vol. 33, no. 12, pp. 2463–2467, Jun. 2015.
- [20] Y. Kim, C. J. Still, D. A. Roberts, and M. L. Goulden, "Thermal infrared imaging of conifer leaf temperatures: Comparison to thermocouple measurements and assessment of environmental influences," *Agricul. Forest Meteorol.*, vol. 248, pp. 361–371, Jan. 2018.
- [21] H. F. Rodrigues, G. Capistrano, F. M. Mello, N. Zufelato, E. Silveira-Lacerda, and A. F. Bakuzis, "Precise determination of the heat delivery during *in vivo* magnetic nanoparticle hyperthermia with infrared thermography," *Phys. Med. Biol.*, vol. 62, no. 10, pp. 4062–4082, May 2017.
- [22] A. D. Gomes, B. Silveira, S. C. Warren-Smith, M. Becker, M. Rothhardt, and O. Frazão, "Temperature independent refractive index measurement using a fiber Bragg grating on abrupt tapered tip," *Opt. Laser Technol.*, vol. 101, pp. 227–231, May 2018.
- [23] Y. Tatsujii, S. Kon, N. Hashimoto, T. Yamaguchi, K. Yazawa, R. Kondo, and K. Kurosawa, "ECT evaluation by an error measurement system according to IEC 60044-8 and 61850-9-2," *IEEE Trans. Power Del.*, vol. 27, no. 3, pp. 1377–1384, Jul. 2012.
- [24] M. K. Rabia, A.-M. Jurdyc, J. Le Brusq, B. Champagnon, and D. Vouagner, "Low frequency Raman scattering for high resolution low temperature optical fiber sensors," *Opt. Laser Technol.*, vol. 94, pp. 25–27, Sep. 2017.
- [25] R. Z. You, L. Ren, and G. Song, "A novel fiber Bragg grating (FBG) soil strain sensor," *Measurement*, vol. 139, pp. 85–91, Jun. 2019.
- [26] L. M. Reindl and I. M. Shrena, "Wireless measurement of temperature using surface acoustic waves sensors," *IEEE Trans. Ultrason., Ferroelectr., Freq. Control*, vol. 51, no. 11, pp. 1457–1463, Nov. 2004.
- [27] A. Kawagoe, K. Hosoda, and J. Tsuruda, "The method to diagnose soundness of the high temperature superconducting coil by pick-up coil pairs," *IEEE Trans. Appl. Supercond.*, vol. 29, no. 5, Aug. 2019, Art. no. 5501504.
- [28] Y. Chen, H. Zhang, and N. Wang, "Body temperature monitor and alarm system used in hospital based on 1-wire and wireless communication technology," in *Proc. Int. Workshop Educ. Technol. Training Int. Workshop Geosci. Remote Sens.*, Shanghai, China, Dec. 2008, pp. 401–404.
- [29] X. Che, D. Nie, P. Tian, and C. Han, "Alarm system for greenhouse temperature management," in *Proc. 2nd Int. Conf. Signal Process. Syst.*, Dalian, China, Jul. 2010, pp. V1-718–V1-721.
- [30] L. Jun, C. Yongqiang, and Y. Mingxin, "The SOPC-based ASF600 wireless temperature measuring system," in *Proc. 2nd IEEE Int. Conf. Inf. Manage. Eng.*, Chengdu, China, Apr. 2010, pp. 612–616.
- [31] X. Y. Chen et al., "Research on temperature compensation method of closed loop all fiber current transformer," *Chin. J. Sens. Actuator*, vol. 32, no. 4, pp. 576–579, Apr. 2019.
- [32] F. F. Sun et al., "A novel fiber Bragg grating ac current transformer with temperature-compensation," *J. Optoelectronic Lase*, vol. 32, no. 4, pp. 576–579, Apr. 2019.
- [33] H. Wang, Y. Guan, Z. Xu, and D. Liu, "Temperature error suppression and compensation technology of fiber optic current transformer," in *Proc. 12th IET Int. Conf. AC DC Power Transmiss. (ACDC)*, Beijing, China, May 2016, pp. 1–3.
- [34] K.-L. Chen, Y.-R. Chen, Y. P. Tsai, and N. Chen, "A novel wireless multifunctional electronic current transformer based on ZigBee-based communication," *IEEE Trans. Smart Grid*, vol. 8, no. 4, pp. 1888–1897, Jul. 2017.
- [35] *Instrument Transformers—Part 2: Additional Requirements for Current Transformers*, Standard IEC 61869-2, 2012.
- [36] *Instrument Transformers—Part: Additional Requirements for Inductive Voltage Transformers*, Standard IEC 61869-3, 2011.



ZHENHUA LI received the B.Sc. degree in biotechnology and the Ph.D. degree in electric engineering from the Huazhong University of Science and Technology, China, in 2008 and 2014, respectively. He is currently an Associate Professor with China Three Gorges University, Yichang, China. His research interests include the condition monitoring of aircraft electric power source, electromagnetic compatibility, energy measurement, approximation algorithm, and fault diagnosis.



Yawei Du received the B.Sc. degree in electrical engineering and automation from the Zhongyuan University of Technology, China, in 2017. He is currently pursuing the master's degree with China Three Gorges University, Yichang, China. His research interests include electromagnetic compatibility and fault diagnosis.



Zhenxing Li received the B.Sc. degree from Hunan University, Changsha, China, in 2000, and the M.Sc. and Ph.D. degrees from the Huazhong University of Science and Technology, Wuhan, China, in 2009 and 2013, respectively. He is currently a Professor with the School of Electrical and New energy, China Three Gorges University, Yichang, China. His major research interests include system protection and smart substation.



A. Abu-Siada (M'07–SM'12) received the B.Sc. and M.Sc. degrees in electrical engineering from Ain Shams University, Egypt, in 1998, and the Ph.D. degree from Curtin University, Australia, in 2004, where he is currently an Associate Professor with the Department of Electrical and Computer Engineering. His research interests include power electronics, power system stability, condition monitoring, and power quality. He is the Editor-in-Chief of the *International Journal of Electrical and Electronic Engineering* and a regular Reviewer of various IEEE TRANSACTIONS. He is the Vice-Chair of the IEEE Computation Intelligence Society and the WA Chapter.



Tao Zhang received the B.S. degree in computer science and technology from Henan Polytechnic University, China, in 2004, and the Ph.D. degree in electric engineering from Fuzhou University, China, in 2010. He is currently an Associate Professor with China Three Gorges University, Yichang, China. His current research interests include condition monitoring and fault diagnosis of power equipment, dielectric measurement, and the optimization of power systems.

• • •